Receiver-Based Localization and Estimation of Polarization Dependent Loss

Alix May[1,2], Elie Awwad[2], Petros Ramantanis[1], Philippe Ciblat[2]
(1) Nokia Bell Labs, 91620 Nozay, France, (2) Télécom Paris, Institut Polytechnique de Paris, 91120 Palaiseau, France
alix.may@nokia.com

Abstract: *We propose a receiver-based estimator of changes in polarization-dependent loss (PDL) values of optical elements. We demonstrate that a PDL as low as 0.25dB can be localized, estimated and distinguished from a polarization-independent loss.*
Keywords: *Non-linear effects, Optical monitoring, Estimation, Polarization dependent loss.*

I. INTRODUCTION

Establishing a lucid diagnosis of an optical network, such as monitoring polarization dependent loss (PDL) can be beneficial for multiple reasons. It enables a careful troubleshooting and better decision making. For instance, whether the detected anomaly is a pure power loss or PDL, the way to adapt the power margin [1] or the modulation and coding scheme might differ. If moderate to high PDL values are detected, a unitary transformation of the polarization tributaries at the transmitter side can help in reducing the bit-error-rate degradation induced by PDL without an increase in the average transmitted power [2]. Some optical components have a polarization-dependent behaviour, which may also change with wavelength, time or their operating point. For instance, a wavelength selective switch (WSS) exhibits a PDL that does not depend only on the wavelength but also on the applied attenuation values per frequency slot [3]. PDL of one WSS can range from 0 to 1dB between an input port and output port. As another example, optical amplifiers such as Erbium doped fibre amplifiers (EDFA) also show a polarization dependent behaviour as their gain value slightly depends on the input polarization state of the optical signal.

In this paper, we introduce a receiver-based method to estimate on-the-field PDL variations of an optical element with respect to precomputed levels obtained from an initial characterization of the components in the network. This method relies on a power profile estimation proposed in [4]. Transceiver-based techniques for optical network monitoring are an interesting approach, because they do not require the addition of extra hardware to monitor the performance. While we chose the approach in [4,5] mainly for the low-complexity digital signal processing (DSP) at the receiver side, other power profile estimation techniques have been suggested in [6] and [7]. A recent work [8] demonstrated the localization of a PDL element using the approach in [4]. In this work, we extend the estimation method of [5] and show that we are able to evaluate changes in the value of a PDL element in an optical transmission system as well as localizing the element.

II. SYSTEM MODEL AND PROPOSED MONITORING SCHEME

To model the impact of an element with a PDL value of ρ_{dB}, defined as the power ratio between the lowest loss and the highest loss expressed in dB, on the incident field, we use the Jones formalism:

$$\begin{pmatrix} E_{x,out} \\ E_{y,out} \end{pmatrix} = Mat_R(\theta,\beta)^{-1} \begin{pmatrix} 1 & 0 \\ 0 & \epsilon \end{pmatrix} Mat_R(\theta,\beta) \begin{pmatrix} E_{x,in} \\ E_{y,in} \end{pmatrix} \quad (1)$$

where $Mat_R(\theta,\beta) = \begin{pmatrix} \cos(\beta) & j\sin(\beta) \\ -j\sin(\beta) & \cos(\beta) \end{pmatrix} \begin{pmatrix} \cos(\theta) & \sin(\theta) \\ -\sin(\theta) & \cos(\theta) \end{pmatrix}$. The angles θ and β describe the eigen polarization directions of the PDL element and $\epsilon = 10^{-\frac{\rho_{\mathrm{dB}}}{20}}$. The PDL estimation is based on the analysis of samples collected at the coherent receiver. It relies on a power profile evaluation [4] that we adapt to detect a PDL, and on a calibration to estimate the value of the PDL element as done in [5] for the power loss. In [4], the evaluated power profile is the sum of the two profiles computed for each polarization tributary. Here, we propose to analyze each profile from each tributary separately.

We illustrate in Fig.1 the new method over the simulated link. The considered optical line is composed of three 100-km spans. The transmission consists in a single polarization division multiplexed quadrature phase-shift keying (PDM-QPSK) channel modulated at 32 GBaud with an input power of 5 dBm. To simulate the propagation in the fibre, we use a split-step Fourier algorithm in Manakov mode with the parameters of a standard single mode fiber (SSMF); the attenuation coefficient is $\alpha_{\mathrm{dB}} = 0.2$ dB/km, the non-linear refraction index $2.5.10^{-20}$ m^2/W and the effective core area is 80 µm^2 at 1550 nm. EDFAs are set to constant output power mode and add an amplified spontaneous emission (ASE) noise with a noise figure equal to 5 dB. Each fibre span is modelled as the product of N = 500 independent waveplates with a polarization mode dispersion (PMD) parameter equal to $PMD = 0.1\ \mathrm{ps}/\sqrt{\mathrm{km}}$. More precisely, each wave-plate of length L_{wp} is represented by the product of the following matrices $Mat_R^{-1}(\theta_i,\beta_i)H_{PMD}Mat_R(\theta_i,\beta_i),\ i = \{1,N\}$ where $H_{PMD} = \mathrm{diag}[\exp(j\,\omega\tau/2), \exp(-j\,\omega\tau/2)]$, ω is the angular frequency and $\tau = PMD\sqrt{L_{wp}}$.

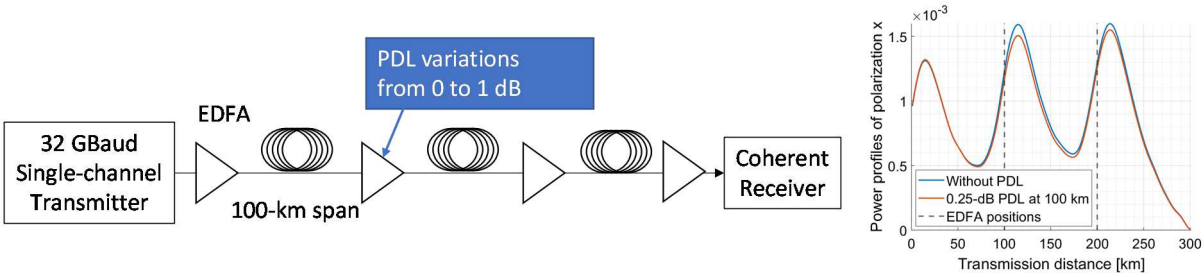

Figure 1: Simulated optical transmission line: 3-span or 8-span (left). Reference and monitoring power profiles of x polarization $P_{ref,x}$ and $P_{mon,x}$ in absence and presence of a 0.25 dB PDL element at 100 km (right).

A variable PDL element is located at the beginning of the second span, to mimic a PDL in a WSS or an EDFA. At the receiver side, after equalization, we perform the power profile estimation per polarization in a similar but non-identical way as [4]. Particularly, the phase rotation that partially compensates the nonlinear self-phase modulation is computed by only considering the power of the corresponding polarization tributary instead of the total power. We first compute two reference power profiles for each polarization $P_{x,ref}$ and $P_{y,ref}$. We aim at monitoring a possible PDL variation with respect to this reference. In our simulation, the reference configuration is PDL-free. During the monitoring phase, we compute the current power profiles and denote them $P_{x,\mathrm{mon}}$ and $P_{y,\mathrm{mon}}$. An example of the reference and monitored power profiles for x-polarization is given in Fig.1 for a PDL-free case and a PDL of 0.25dB. Now to detect a change in PDL, we focus on the anomaly indicator $AI_i = P_{i,ref} - P_{i,mon}$, $i = \{x, y\}$. In Fig.2a and b, we plot the anomaly indicators for polarization x and polarization y respectively, for three different incident states of the signal at the PDL element with $\rho_{\mathrm{dB}} = 0.25$dB. The considered state-of-polarization (SOP) evolutions of the signal from the transmitter output to the PDL element reduce to one Mat_R with $\theta = \{0, \frac{\pi}{4}, \frac{\pi}{2}\}$ and β set to zero. By looking at the first half of the figures, the peaks are located around the position of the amplifier at 100km, i.e., around the position of the PDL element. More accurately, the position of a power anomaly is given by the position of the maximum slope of the anomaly indicator as shown in [4]. We see that the peak amplitudes in Fig.2a and Fig.2b are perfectly correlated to the incident signal's SOP. Indeed, without PDL ($\epsilon = 1$), from Eq.(1), we get $P_{x,out,ref} = P_{y,out,ref} = \frac{P_0}{2}$ where $P_0 = |E_{x,in}|^2 + |E_{y,in}|^2$. While in presence of non-zero PDL, $P_{x,out,mon} = \frac{P_0}{2}(\cos^2(\theta) + \epsilon^2 \sin^2(\theta))$ and $P_{y,out,mon} = \frac{P_0}{2}(\sin^2(\theta) + \epsilon^2 \cos^2(\theta))$ yielding $P_{out,mon} = \frac{P_0}{2}(1 + \epsilon^2)$. Hence, for $\theta = 0$, the lost power according to the PDL model is equal to $P_{x,out,ref} - P_{x,out,mon} = 0$ for x polarization and $P_{y,out,ref} - P_{y,out,mon} = \frac{P_0}{2} \cdot (1 - \epsilon^2)$, confirming that x-polarization did not lose any power between the reference and the monitoring configurations while the y-polarization loses power and shows the highest AI_y peak. The opposite behaviour is obtained for $\theta = \frac{\pi}{2}$ for which the x-polarization endures all the power loss. We can also check that the two polarization tributaries lose the same power for $\theta = \frac{\pi}{4}$.

Now, we examine the secondary peaks observed in the simulated AI. To understand their occurrence, we show, in Fig. 2c, the sum of the anomaly indicators per polarization: $AI = AI_x + AI_y$. We can see a peak located at the position of the PDL element, but no additional peak. The first one indicates that there is a power loss at that position and its height relates to the total power loss between the reference configuration without PDL and the monitoring phase with PDL: $P_{x,out,ref} + P_{y,out,ref} - (P_{y,out,mon} + P_{x,out,mon}) = \frac{P_0}{2}(1 - \epsilon^2)$. The absence of secondary peaks around 200 km is due to the operation mode of the amplifiers set to the constant output power mode. The additional loss due to the PDL element is fully compensated by the amplifier so that the power at 200 km is the same as the one in the reference configuration, which explains the absence of a peak. However, since the amplifiers compensate for the total loss regardless of the polarization dependence of endured losses, the mismatch between the polarizations is not compensated. Therefore, the

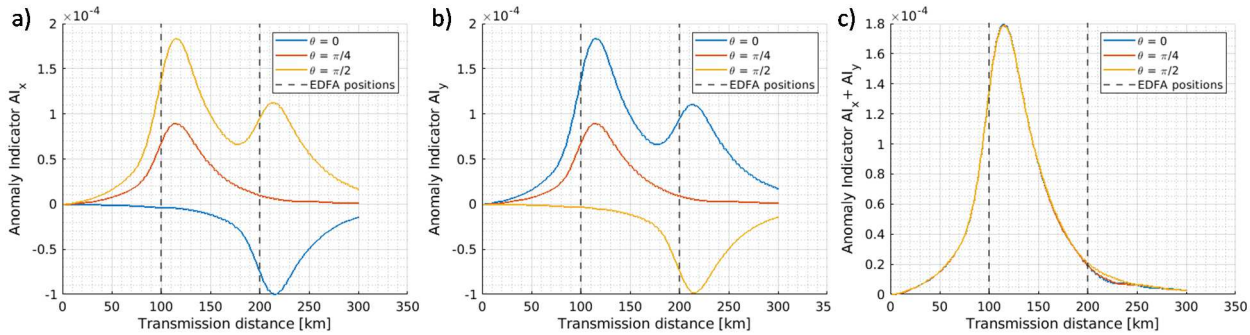

Figure 2: Anomaly indicators over x-polarization AI_x (a), y-polarization AI_y (b) and both AI (c) in presence of PDL.

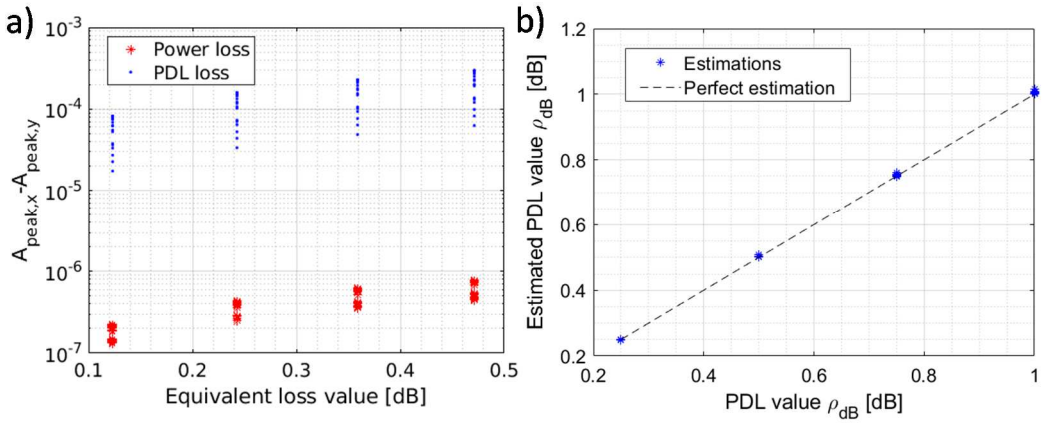

Figure 3: (a) Difference between AI_x and AI_y peaks when a PDL (blue) or a power loss is introduced (red) in the link. (b) Estimated PDL values versus function of inserted PDL values. For each value, 20 estimations for 20 SOP values.

power at 200km after compensation is different for each polarization compared to the reference case. This explains the occurrence of the secondary peaks and their symmetry with respect to the horizontal axis in Fig. 2a and b.

III. IMPLEMENTATION AND PERFORMANCE

In this section, we comment on the extraction of the power loss factor from the *AI* and we demonstrate the ability of our estimator to reveal the polarization dependence of the detected loss and measure the PDL value. We first recall the model we proposed in [5] to estimate a power loss value $(1-T)$ from the *AI* peak amplitude A_{peak}:

$$A_{\text{peak}}(1-T, d_l) = C_{\text{calib}} \cdot (1-T) \cdot 10^{-\frac{\alpha_{\text{dB}}}{10} \cdot d_l} \qquad (2)$$

where d_l is the unknown distance between the power loss and the previous amplifier and C_{calib} is the calibration factor. In [5], we determine this calibration factor by varying the output power of the amplifier – mimicking a power loss value $(1-T)$ – and determining the slope of the function $A_{\text{peak}}(1-T, d_l = 0)$. The unknown distance d_l of the power loss from the amplifier is estimated using the position of the maximum slope of the detected *AI* peak and the position of the amplifier given by the calibration step. In the PDL case, it is the height of the peak in the sum of AI_x and AI_y (see Fig.2c) which is linked to the value ρ_{dB} of the PDL element. Based on the PDL model proposed in section II, the loss factor in the PDL case is $\frac{(1-\epsilon^2)}{2}$. Therefore, Eq. (2) can be now written as:

$$A_{\text{peak}} = C_{\text{calib}} \cdot \frac{1-\epsilon^2}{2} \cdot 10^{-\frac{\alpha_{dB}}{10} \cdot d_l} \qquad (3)$$

From (3), we see that the same calibration procedure as in [5] can be used to estimate ρ_{dB}. To determine d_l, a similar approach as described before can be used. However, since PDL is due to components in nodes or amplifiers and not distributed in the fiber itself, it can be fair to set this distance to zero if its determined value is small.

First, we test the differentiation capability between a polarization-dependent and a polarization-independent loss by inserting a PDL element or a polarization-independent extra loss at the beginning of the second span of Fig.1. PDL values are set to $\rho_{dB} = \{0.25, 0.5, 0.75, 1\}$ dB while, to compare equivalent power losses, the polarization-independent losses are chosen so that the loss factors are equal in both cases: $(1-T) = (1-\epsilon^2)/2$. In Fig. 3a, we show the difference between the peaks in the anomaly indicators AI_x and AI_y over 20 random fiber states for both loss types and for four loss levels. We see that the PDL can be clearly distinguished as the values of the peak differences are almost 100 times higher in the case of a PDL event. In practice, by setting an arbitrary threshold to 10^{-5}, we can see that we would distinguish the two types of losses perfectly. Next, we assess the accuracy in estimating ρ_{dB} for the link configuration in Fig.1. We plot in Fig. 3b, for each ρ_{dB}, 20 makers corresponding to the estimations for 20 random SOPs. The estimator offers high accuracy even for PDL levels as low as 0.25 dB. Indeed, for 3 spans, the standard deviation obtained is 0.0033 dB for $\rho_{\text{dB}} = 1$ dB. When we increase the number of spans to 8, we get a slightly higher standard deviation of 0.0038 dB. In addition, the PDL element was perfectly localized at the position of the amplifier of interest in all cases. This is the type of location accuracy that we obtained in experiments when the loss was located at the position of the amplifier, where the power is the highest [5]. Note that, in both cases, the step chosen is 1km, therefore the maximum accuracy achieved is 1km.

IV. CONCLUSION

We proposed a receiver-based method to detect, estimate and localize PDL in a multi-span optical link. We showed that it was possible to differentiate a polarization-dependent from a polarization-independent loss. Finally, we obtained excellent estimation accuracy on PDL values ranging from 0.25 to 1 dB. The location of the element whose PDL was varied was estimated with a precision of 1 km, which can give good insights on the relevant element.

REFERENCES

[1] J. Girard-Jollet *et al.*, 'Estimating Network Components Polarization-Dependent Loss Using Performance Statistical Measurements', in *2021 European Conference on Optical Communication (ECOC)*, Bordeaux, France, Sep. 2021, pp. 1–4. doi: 10.1109/ECOC52684.2021.9606155.

[2] A. Dumenil *et al.*, 'PDL in Optical Links: A Model Analysis and a Demonstration of a PDL-Resilient Modulation', *J. Lightwave Technol.*, vol. 38, no. 18, pp. 5017–5025, Sep. 2020, doi: 10.1109/JLT.2020.2998841.

[3] D. Xie *et al.*, 'LCoS-Based Wavelength-Selective Switch for Future Finer-Grid Elastic Optical Networks Capable of All-Optical Wavelength Conversion', *IEEE Photonics J.*, vol. 9, no. 2, pp. 1–12, Apr. 2017, doi: 10.1109/JPHOT.2017.2671436.

[4] T. Tanimura *et al.*, 'Fiber-Longitudinal Anomaly Position Identification Over Multi-Span Transmission Link Out of Receiver-end Signals', *J. Lightwave Technol.*, vol. 38, no. 9, pp. 2726–2733, 2020, doi: 10.1109/JLT.2020.2984270.

[5] A. May *et al.*, 'Receiver-Based Experimental Estimation of Power Losses in Optical Networks', *IEEE Photon. Technol. Lett.*, vol. 33, no. 22, pp. 1238–1241, 2021, doi: 10.1109/LPT.2021.3115627.

[6] T. Sasai *et al.*, 'Simultaneous Detection of Anomaly Points and Fiber types in Multi-span Transmission Links Only by Receiver-side Digital Signal Processing', in *Optical Fiber Communication Conf.*, San Diego, California, 2020, p. Th1F.1. doi: 10.1364/OFC.2020.Th1F.1.

[7] S. Gleb *et al.*, 'Fiber Link Anomaly Detection and Estimation Based on Signal Nonlinearity', *European Conference on Optical Communication*, p. Tu2C2.5, 2021.

[8] M. Eto *et al.*, 'Location-Resolved PDL Monitoring With Rx-Side Digital Signal Processing in Multi-Span Optical Transmission Systems', in *Optical Fiber Communication Conf.*, San Diego, California, 2022, p. Th1C.2.